# Effect of the body position on natural convection within the anterior chamber of the human eye during exposure to electromagnetic fields

Teerapot Wessapan, Phadungsak Rattanadecho & Patcharaporn Wongchadakul

Published online: 22 Mar 2016.

Submit your article to this journal ↗

View related articles ↗

View Crossmark data ↗

Taylor & Francis
Taylor & Francis Group

# Effect of the body position on natural convection within the anterior chamber of the human eye during exposure to electromagnetic fields

Teerapot Wessapan[a], Phadungsak Rattanadecho[b], and Patcharaporn Wongchadakul[b]

[a]School of Aviation, Eastern Asia University, Rungsit, Thanyaburi, Pathumthani, Thailand; [b]Center of Excellence in Electromagnetic Energy Utilization in Engineering (CEEE), Department of Mechanical Engineering, Faculty of Engineering, Thammasat University (Rangsit Campus), Khlong Nueng, Khlong Luang, Pathumthani, Thailand

## ABSTRACT

Heating is the main biological effect of the electromagnetic (EM) fields to human eye. This study intends to focus attention on the differences in the heat transfer characteristics of the human eye induced by EM fields in different body positions. The effect of three different body positions – sitting, supine, and prone – on natural convection of aqueous humor (AH) in the anterior chamber of the eye is systematically investigated. The specific absorption rate (SAR) value, fluid flow, and the temperature distribution in the eye during exposure to EM fields are obtained by numerical simulation of EM wave propagation. In this study, the frequencies of 900 and 1,800 MHz are chosen for the investigations. The heat transfer model used in this study is developed based on natural convection and porous media theories. The results show that the AH temperature inside the anterior chamber is the highest in the supine position at both frequencies. It is found that during exposure to EM fields, body position plays an important role on AH natural convection and the heat transfer process within the anterior chamber and its periphery in the front part of the eye. However, the body position has no significant effect on temperature distribution for the middle part of the eye. The obtained results provide information on the body position and thermal effects from EM fields exposure.

## 1. Introduction

In the eye, the natural convection is caused by buoyancy effects arising from the gravity force on density differences in a body of the AH in the anterior chamber. The cornea is cooled by the air and tears the evaporation film. This convective flow of the AH is influenced by the difference in temperature between the external cornea and the internal lens. Moreover, the AH natural convection induced by the intense electromagnetic (EM) fields has a significant impact on the temperature increase within the anterior chamber [1–3]. Intense exposure to EM fields causes heating of tissues with potentially harmful effects. It is well known that the eye is one of the organs most sensitive to environmental factors such as EM fields. Recommendations that limit the exposure have been issued by the International Commission on Non-Ionizing Radiation Protection (ICNIRP 1998) [4] and the Institute of Electrical and Electronics Engineers (IEEE 2005) [5]. Normally natural convection is highly dependent on the geometry of the hot surface. Therefore the changes in body position that change the anterior chamber orientation could have a significant effect on the convective flow of the AH. Moreover, body position also affects the natural convection in the eye, especially when subjected to EM fields.

## Nomenclature

| | | | | |
|---|---|---|---|---|
| $C$ | specific heat capacity (J/(kg K)) | | $\varepsilon$ | permittivity (F/m) |
| $E$ | electric field intensity (V/m) | | $\sigma$ | electric conductivity (S/m) |
| $e$ | tear evaporation heat loss (W/m$^2$) | | $\omega$ | angular frequency (rad/s) |
| $f$ | frequency of incident wave (Hz) | | $\rho$ | density (kg/m$^3$) |
| $H$ | magnetic field (A/m) | | $\omega_b$ | blood perfusion rate (1/s) |
| $h$ | convection coefficient (W/m$^2 \cdot$K) | | $\Gamma$ | external surface area |
| $j$ | current density (A/m$^2$) | | | |
| $k$ | thermal conductivity (W/(m K)) | | **Subscripts** | |
| $n$ | normal vector | | $am$ | ambient |
| $p$ | pressure (N/m$^2$) | | $b$ | blood |
| $Q$ | heat source (W/m$^3$) | | $ext$ | external |
| $T$ | temperature (K) | | $i$ | subdomain |
| $u$ | velocity (m/s) | | $met$ | metabolic |
| $t$ | time | | $r$ | relative |
| $B$ | volume expansion coefficient (1/K) | | $ref$ | reference |
| $\mu$ | magnetic permeability (H/m) | | 0 | free space, initial condition |

Several numerical models of the eye heat transfer have been investigated to illustrate the temperature distribution in the eye in different environmental conditions. At the beginning, most studies of heat transfer analysis in human tissue, especially in the eye, used heat conduction equations [6–12]. Some studies were carried out on the natural convection in the eye based on heat conduction models [13, 14]. Ooi and Ng [14, 15] studied the effect of aqueous humor (AH) hydrodynamics on heat transfer in the eye based on a heat conduction model. Meanwhile, the bioheat equation, introduced by Pennes [16, 17], based on the heat diffusion equation for a blood perfused tissue, was used for modeling the heat transfer in the eye as well [18, 19]. Ooi and Ng also developed a 3D model of the eye [20], extending their 2D model [18]. Recently, porous media models have been utilized to investigate the transport phenomena in biological media instead of a simplified bioheat model [21–23]. Shafahi and Vafai [24] proposed porous media along with a natural convection model to analyze the eye thermal characteristics during exposure to thermal disturbances. Advanced models of the eye based on natural convection theory have been used in the various applications [25–33]. Ooi et al. and Tan et al. conducted advanced numerical modeling of the human eye based on the boundary element method [29–33]. Furthermore, Heussuer et al. [34] developed a numerical model that includes a vertical blood stream in the choroid.

Our research group has numerically investigated the temperature increase in human tissue subjected to EM fields in several problems [1–3, 35–41]. Wessapan et al. [1–3] investigated the SAR and temperature distributions in the eye during exposure to EM waves using the porous media theory. Wessapan et al. [35, 36] utilized a 2D finite element method (FEM) to obtain the specific absorption rate (SAR) and temperature increase in the human body exposed to leaked EM waves. Wessapan et al. [37, 38] developed a 3D model of the human head in order to investigate the SAR and temperature distributions in the human head during exposure to mobile phone radiation. Keangin et al. [39–41] carried out a numerical simulation of a liver cancer treatment using a complete mathematical model that considered the coupled model of EM wave propagation, heat transfer, and mechanical deformation in the biological tissue in the couple's way.

However, most studies have mainly focused on the modeling and the influence of the external conditions, but they have not considered the effects of eye geometry configuration such as body position and anterior chamber orientation in the simulations, although it directly affects heat transfer from the eye surface. In practical situations, these effects lead to enhanced convection heat transfer within the anterior chamber, which can cause changes in temperature to the eye. Therefore, in order to provide adequate information on the levels of exposure and health effects from EM fields' exposure, it is essential to consider the effect of body position in the analysis.
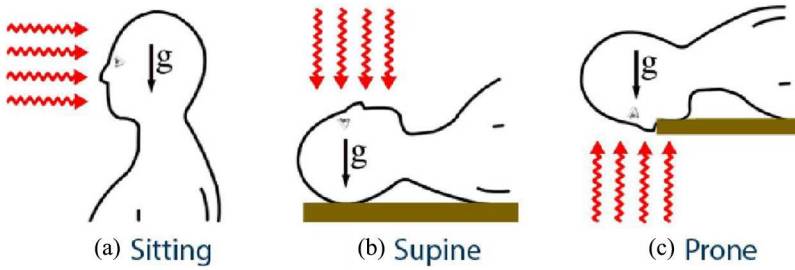
Figure 1. Human eye exposure to EM radiation in different body positions.

This study presents the simulation of the SAR, fluid flow, and temperature distributions in an anatomical human eye exposed to EM fields in different body positions. The work described in this paper is substantially extended from our previous work [1–3] by further enhancing the focus on the effect of change in body position on natural convection within the anterior chamber. A 2D heterogeneous human eye model is used to simulate the SAR, fluid flow, and temperature distributions in the eye model. The EM wave propagation in the eye is expressed mathematically by Maxwell's equations. The analysis of heat transfer is investigated using a recently developed heat transfer model based on natural convection and porous media theory [24]. In the heterogeneous eye model, the effect of three different body positions – sitting, supine, and prone – on natural convection in the anterior chamber of the eye is systematically investigated. The SAR, fluid flow, and temperature distributions in the eye during exposure to EM fields of 900 and 1,800 MHz are obtained by numerical simulation of the EM wave propagation and heat transfer equations. The eye model excluded the presence of the eyelid as well as the metabolic heat generation in order to ease the modeling procedures.

## 2. Formulation of the problem

It is well known that the eye consists primarily of water, especially the AH in the anterior chamber. When the eye is exposed to EM fields, the temperature gradient within the anterior chamber plays an important role in AH natural convection. This study investigates the effect of body position on natural convection in the anterior chamber when subjected to EM fields. Figure 1 shows human eye exposure to EM radiation in different body positions. Owing to ethical consideration, exposing the human to EM fields for experimental purposes is limited. It is more convenient to develop a realistic human eye model through the numerical simulation. A highlight of this work is the illustration of the transport phenomena, including the heat and mass transfer in the eye during exposure to EM fields in different body positions. The analyses of the SAR, heat transfer, and fluid flow in the eye exposed to EM fields will be illustrated in Section 3. The system of governing equations as well as the initial and boundary conditions are solved numerically using the FEM.

## 3. Methods and model

This study focuses on the differences in heat transfer characteristics of the human eye induced by EM fields in different body positions. The first step in evaluating the effects of a certain exposure to EM fields in the eye is to determine the induced internal EM fields and its spatial distribution. Thereafter, EM energy absorption, which results in a temperature increase in the eye and other processes of transport phenomena, can be considered.

### 3.1. Physical model

A 2D model of the eye, which follows the physical model in the previous research [24], is developed. Figure 2 shows the 2D eye model used in this study. This model comprises seven types of tissue: the
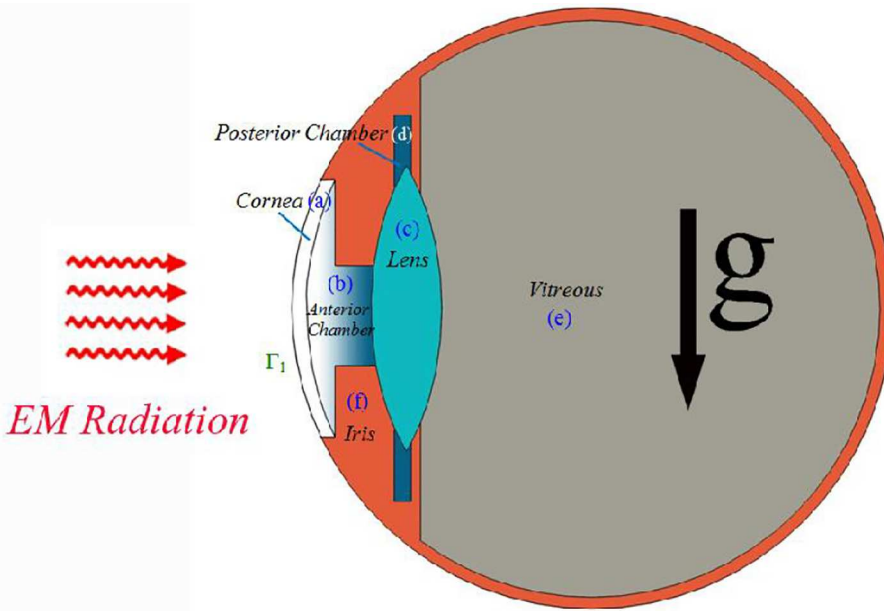
**Figure 2.** Human eye model vertical cross section [24].

cornea, anterior chamber, posterior chamber, iris, sclera, lens, and vitreous. These tissues have different dielectric and thermal properties. In the sclera layer, there are two more layers known as the choroid and retina, which are relatively thin compared to the sclera. To simplify the problem, these layers are assumed to be homogenous. The iris and sclera, which have the same properties, are modeled together as one homogenous region. The dielectric and thermal properties of tissues are given in Tables 1 and 2, respectively. Each tissue is assumed to be homogeneous and electrically as well as thermally isotropic.

## 3.2. Equations for EM wave propagation analysis

The mathematical models are developed to predict the electric fields and the SAR with respect to the temperature gradient in the eye. To simplify the problem, the following assumptions are made:
1. The EM wave propagation is modeled in two dimensions.
2. The eye in which the EM waves interact with the eye proceeds in the open region.
3. The free space is truncated by scattering boundary condition.
4. The model assumes that dielectric properties of each tissue are constant.
5. In the eye, the EM waves are characterized by transverse magnetic fields (TM-mode).

**Table 1.** Dielectric properties of tissues at 900 MHz and 1,800 MHz [42, 43].

| Tissue | Frequency: 900 MHz | | Frequency: 1,800 MHz | |
|---|---|---|---|---|
| | $\varepsilon_r$ | σ (S/m) | $\varepsilon_r$ | σ (S/m) |
| Cornea (a) | 52.0 | 1.85 | 55.0 | 2.32 |
| Anterior Chamber (b) | 73.0 | 1.97 | 75.0 | 2.40 |
| Lens (c) | 51.3 | 0.89 | 41.1 | 1.29 |
| Posterior Chamber (d) | 73.0 | 1.97 | 75.0 | 2.40 |
| Vitreous (e) | 74.3 | 1.97 | 73.7 | 2.33 |
| Sclera (f) | 52.1 | 1.22 | 52.7 | 1.68 |
| Iris (f) | 52.1 | 1.22 | 52.7 | 1.68 |

**Table 2.** Thermal properties of the eye [14].

| Tissue | ρ (kg/m³) | k (W/m°C) | $C_p$ (J/kg°C) | μ (N s/m²) | β (1/K) |
|---|---|---|---|---|---|
| Cornea (a) | 1,050 | 0.58 | 4,178 | – | – |
| Anterior Chamber (b) | 996 | 0.58 | 3,997 | 0.00074 | 0.000337 |
| Lens (c) | 1,000 | 0.4 | 3,000 | – | – |
| Posterior Chamber (d) | 996 | 0.58 | 3,997 | – | – |
| Vitreous (e) | 1,100 | 0.603 | 4,178 | – | – |
| Sclera (f) | 1,050 | 1.0042 | 3,180 | – | – |
| Iris (f) | 1,050 | 1.0042 | 3,180 | – | – |

The EM wave propagation in the eye in Figure 2 is calculated using Maxwell's equations, which mathematically describe the interdependence of the EM waves. The general form of Maxwell's equations is simplified to demonstrate the EM fields penetrated in the eye as the following equation:

$$\nabla \times \left( \left( \varepsilon_r - \frac{j\sigma}{\omega\varepsilon_0} \right)^{-1} \nabla \times H_z \right) - \mu_r k_0^2 H_z = 0 \tag{1}$$

where $H$ is the magnetic field (A/m), $\mu_r$ is the relative magnetic permeability, $\varepsilon_r$ is the relative dielectric constant, $\varepsilon_0 = 8.8542 \times 10^{-12}$ F/m is the permittivity of free space, and $k_0$ is the free space wave number (m⁻¹).

### 3.2.1. Boundary condition for wave propagation analysis

EM energy is emitted by an EM radiation device and falls on the eye with a particular power density. Therefore, the boundary condition for solving EM wave propagation, as shown in Figure 3, is described as follows:

It is assumed that the uniform wave flux falls on the left side of the eye. Therefore, at the left boundary of the considered domain, an EM simulator employs TM wave propagation port with specified power density:

$$S = \int (E - E_1) \cdot E_1 / \int E_1 \cdot E_1 \ dA_1 \tag{2}$$
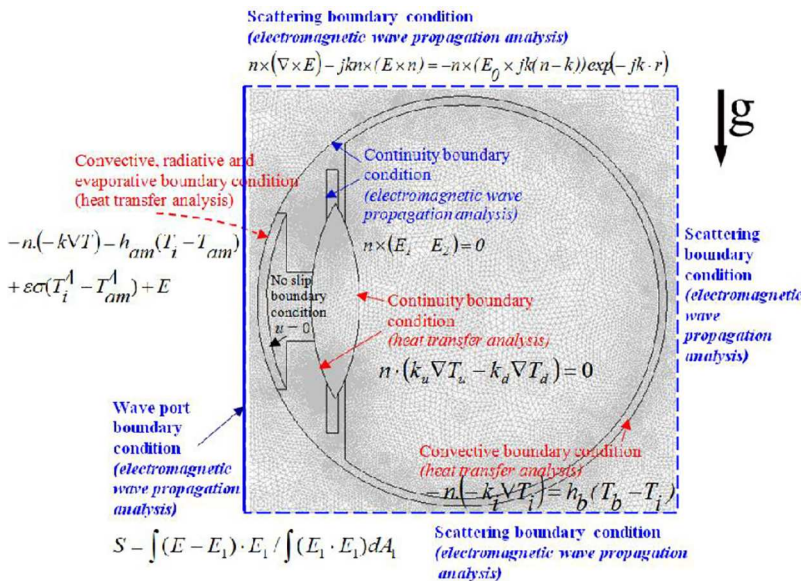


**Figure 3.** Boundary condition for analysis with a 2D finite element mesh of the eye model.

Boundary conditions along the interfaces between different mediums, for example, between air and tissue or tissue and tissue, are considered as continuity boundary condition

$$n \times (E_1 - E_2) = 0 \tag{3}$$

The outer sides of the calculated domain, i.e., free space, are considered as scattering boundary condition:

$$n \times (\nabla \times E_z) - jkE_z = -jk(1 - k \cdot n)E_{0z} \exp(-jk \cdot r) \tag{4}$$

where $k$ is the wave number (m$^{-1}$), $\sigma$ is the electrical conductivity (S/m), $n$ is the normal vector, $j = \sqrt{-1}$, and $E_0$ is the incident plane wave (V/m).

### 3.3. Interaction of EM fields and human tissues

Interaction of EM fields with biological tissue can be defined in terms of SAR. When the EM waves propagate through the tissue, the energy of EM waves is absorbed by the tissue. The SAR is defined as the power dissipation rate normalized by material density [23]. The SAR is given by

$$SAR = \frac{\sigma}{\rho}|E|^2 \tag{5}$$

where $E$ is the electric field intensity (V/m), $\sigma$ is the electric conductivity (S/m), and $\rho$ is the tissue density (kg/m$^3$).

### 3.4. Equations for heat transfer and flow analysis

To solve the thermal problem, a coupled effect of the EM wave propagation and the unsteady bioheat transfer are investigated. The temperature distribution corresponds to the SAR. This is because the SAR in the eye distributes owing to energy absorption. Thereafter, the absorbed energy is converted to thermal energy, which increases the tissue temperature.

Heat transfer analysis of the eye is modeled in two dimensions. To simplify the problem, the following assumptions are made:
1. The human tissue is a biomaterial with constant thermal properties.
2. There is no phase change of substance in the tissue.
3. There is a local thermal equilibrium between the blood and the tissue.
4. There is no chemical reaction in the tissue.

This study utilized the pertinent thermal model based on the porous media theory [24] to investigate the heat transfer behavior of the eye when exposed to the EM fields.

In this study, the motion of fluid is considered only inside the anterior chamber (subdomain $b$ in Figure 2) [14]. There is a blood flow in the iris/sclera part, which plays a role to adjust the eye temperature with the rest of the body. For the rest of the parts, the metabolic heat generation is neglected based on the fact that these comprise mainly water. The equations governing the flow of heat in cornea, posterior chamber, lens, and vitreous resemble the classical heat conduction equation given in Eq. (6):

$$\rho_i C_i \frac{\partial T_i}{\partial t} = \nabla \cdot (k_i \nabla T_i) + Q_{ext}; i = a, c, d, e \tag{6}$$

This model accounts for the existence of AH in the anterior chamber. The heat transfer process consists of both conduction and natural convection, which can be written as follows:

Continuity equation:

$$\nabla \cdot u_i = 0; i = b \tag{7}$$

Momentum equation:

$$\rho_i \frac{\partial u_i}{\partial t} + \rho_i u_i \nabla \cdot u_i = -\nabla p_i + \nabla \cdot [\mu(\nabla u_i + \nabla u_i^T)] + \rho_i g\beta_i(T_i - T_{ref}); i = b \tag{8}$$

where $i$ denotes each subdomain in the eye model as shown in Figure 2, $\rho$ is the tissue density (kg/m$^3$), $\beta$ is the volume expansion coefficient (1/K), $u$ is the velocity (m/s), $p$ is the pressure (N/m$^2$), $\mu$ is the dynamic viscosity of AH (N·s/m$^2$), $t$ is the time, $T$ is the tissue temperature (K), and $T_{ref}$ is the reference temperature considered here, which is 37°C. The effects of buoyancy due to the temperature gradient are modeled using the Boussinesq approximation, which states that the density of a given fluid changes slightly with temperature but negligibly with pressure.

Energy equation:

$$\rho_i C_i \frac{\partial T_i}{\partial t} - \nabla \cdot (k_i \nabla T_i) = -\rho C_i u_i \cdot \nabla T_i + Q_{ext}; i = b \tag{9}$$

The sclera/iris is modeled as a porous medium with blood perfusion, which assumes that local thermal equilibrium exists between the blood and the tissue. The blood perfusion rate used is 0.004 1/s. A modified Pennes' bioheat equation [24] is used to calculate the temperature distribution in the sclera/iris.

$$(1 - \varepsilon)\rho_i C_i \frac{\partial T_i}{\partial t} = \nabla \cdot ((1 - \varepsilon)k_i \nabla T_i) + \rho_b C_b \omega_b (T_b - T_i) + Q_{ext}; i = f \tag{10}$$

where $C$ is the heat capacity of tissue (J/kg K), $k$ is the thermal conductivity of tissue (W/m K), $T_b$ is the temperature of blood (K), $\rho_b$ is the density of blood (kg/m$^3$), $C_b$ is the specific heat capacity of blood (J/kg K), $\omega_b$ is the blood perfusion rate (1/s), and $Q_{ext}$ is the external heat source term (EM heat-source density) (W/m$^3$).

In this analysis, the porosity ($\varepsilon$) used is assumed to be 0.6. The heat conduction between the tissue and the blood flow is approximated by the blood perfusion term $\rho_b C_b \omega_b (T_b - T)$.

The external heat source term is equal to the resistive heat generated by the EM fields (EM power absorbed), which is defined as

$$Q_{ext} = \frac{1}{2} \sigma_{tissue} |\overline{E}|^2 = \frac{\rho}{2} \cdot SAR \tag{11}$$

where $\sigma_{tissue}$ is the electric conductivity of the tissue (S/m).

### 3.4.1. Boundary condition for heat transfer analysis
The heat transfer analysis excluding the surrounding space is considered only in the eye. The corneal surface, shown in Figure 3, is considered under the convective, radiative, and evaporative boundary conditions.

$$-n \cdot (-k\nabla T) = h_{am}(T_i - T_{am}) + \varepsilon\sigma(T_i^4 - T_{am}^4) + e \text{ on } \Gamma_1 \ i = a \tag{12}$$

where $\Gamma_i$ is the external surface area corresponding to section $i$, $e$ is the tear evaporation heat loss (W/m$^2$), $T_{am}$ is the ambient temperature (K), and $h_{am}$ is the convection coefficient (W/m$^2$·K).

The temperature of blood is generally assumed to be the same as the body core temperature, which causes heat to be transferred into the eye [14]. The surface of the sclera is assumed to be under the convective boundary condition

$$-n \cdot (-k_i \nabla T_i) = h_b(T_b - T_i) \text{ on } \Gamma_2 i = f \tag{13}$$

where $h_b$ is the convection coefficient of blood (65 W/m$^2$·K). $\Gamma_1$ and $\Gamma_2$ are the corneal surface and scleral surface of the eye, respectively.

### 3.5. Calculation procedure

In this study, FEM is used to analyze the transient problems. The computational scheme is to assemble finite element model and compute a local heat generation term by performing an EM calculation using tissue properties. In order to obtain a good approximation, a fine mesh is specified in the sensitive areas. This study provides a variable mesh method for solving the problem as shown in Figure 3. The system of governing equations and both the initial and boundary conditions are then solved. All computational processes are implemented using COMSOL™ Multiphysics, to demonstrate the phenomenon that occurs in the eye exposed to the EM fields.

The 2D model is discretized using triangular elements and the Lagrange quadratic is then used to approximate the temperature and SAR variations across each element. A convergence test is carried out to identify the suitable number of elements required. This convergence test leads to a grid with approximately 10,000 elements. It is reasonable to assume that, at this element number, the accuracy of the simulation results is independent of the number of elements.

## 4. Results and discussion

When the eye is exposed to EM fields, the gravity effect on the AH flow and heat transfer will have a different effect depending on the eye orientation, which is relative to the body position. In this study, the AH is considered to be incompressible, steady-state, Newtonian, and the Boussinesq approximation is applied for natural convection with constant physical properties. The AH natural convection of the human eye at different body positions induced by EM fields is systematically investigated. This work focuses on the effect of three different body positions: sitting, supine, and prone on natural convection in the anterior chamber of the eye. The EM frequencies of 900 and 1,800 MHz are chosen for the investigations since they are used in most parts of the world. The coupled model of the EM propagation and thermal as well as fluid fields is solved numerically. For the simulation, the dielectric and thermal properties are directly taken from Tables 1 and 2, respectively.
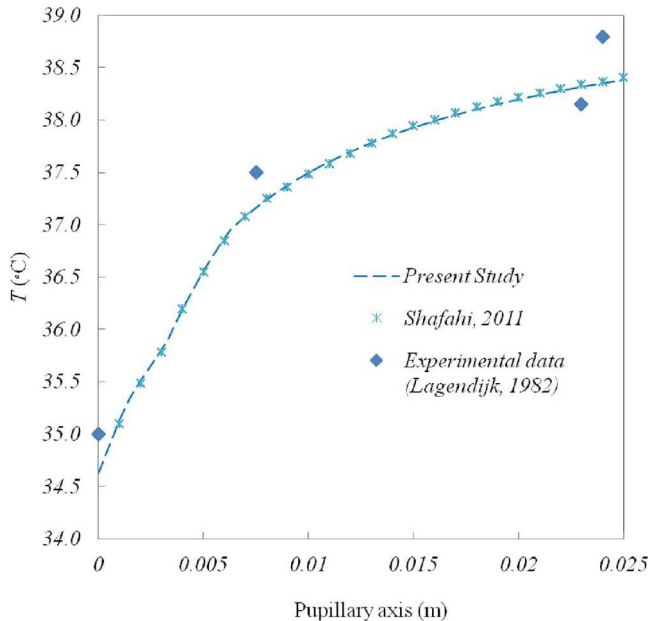


**Figure 4.** Comparison of the calculated temperature distribution to the temperature distribution obtained by Shafahi and Vafai [24], and Lagendijk's experimental data [8]; $h_{am} = 20 \, \text{W/m}^2 \cdot \text{K}$ and $T_{am} = 25°C$.

## 4.1. Verification of the model

To perform verification of the models presented here, the case without EM fields of the simulated results from this study are validated against the numerical results obtained with the same geometric model by Shafahi and Vafai [24]. Moreover, the comparison between experimental results for a rabbit obtained by Lagendijk [6] and the present numerical results has been performed. The validation case assumes that the rabbit body temperature is 38.8°C, the tear evaporation heat loss is 40 W/m², the ambient temperature is 25°C, and the convection coefficient of ambient air is 20 W/m² · K. The results of the selected test case are depicted in Figure 4 for temperature distribution in the eye. The figure clearly shows a good agreement between experimental and numerical temperature distribution in the eye. This favorable comparison ensures that the numerical model can accurately represent the transport phenomena in the eye.

## 4.2. SAR Distribution

Figures 5a and 6a show the SAR distribution evaluated on the vertical cross section of the eye in different body positions during exposure to the EM frequencies of 900 and 1,800 MHz, respectively. The
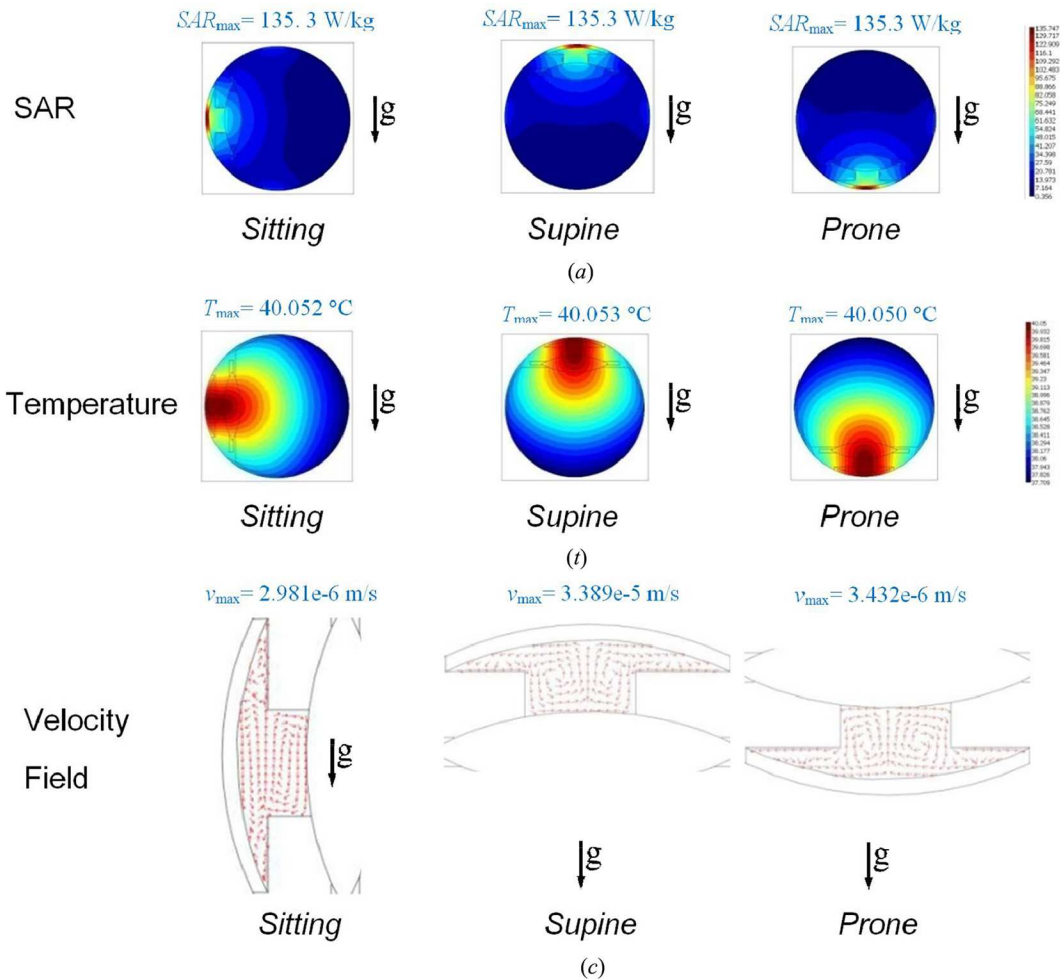


**Figure 5.** The SAR, temperature distribution, and velocity field in the eye at various body positions exposed to the EM power density of 100 mW/cm² at the frequency of 900 MHz.
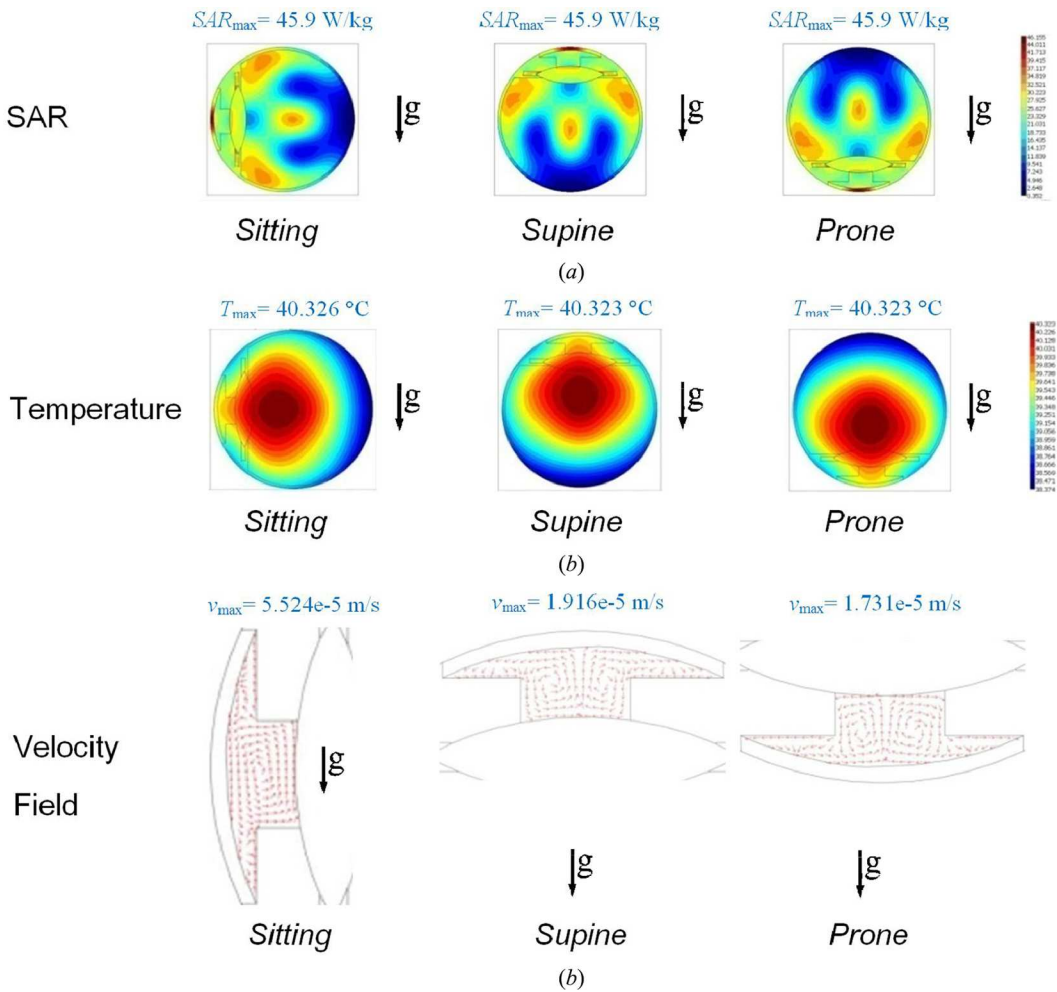
**Figure 6.** The SAR, temperature distribution, and velocity field in the eye in different body positions exposed to the EM power density of 100 mW/cm² at the frequency of 1,800 MHz.

SAR values in the eye are increased corresponding to the electric field intensities. From the previous work [2] at the power density of 100 mW/cm², the maximum electric field intensities of the frequencies of 900 and 1,800 MHz are 391.8 and 231.2 V/m, respectively. Besides the electric field intensity, the magnitude of the dielectric and thermal properties (Tables 1 and 2) in each tissue will directly affect SAR distributions in the eye. For all cases, the highest SAR values are obtained in the region of the corneal surface. For all body positions, the frequencies of 900 and 1,800 MHz display maximum SAR values of 135.2 and 45.9 W/kg, respectively. It is found that the body position has no influence on the SAR values in the eye. This is because gravity has a negligible influence on the EM energy absorption behavior of the eye tissue.

## 4.3. Temperature distributions and velocity fields

Normally natural convection is highly dependent on the geometry of the container surface. Therefore, the changes in body position that change the anterior chamber orientation could have a significant effect on the convective flow of the AH. Moreover, the body position also affects natural convection in the eye, especially when subjected to EM fields. A numerical simulation was carried out to

investigate the temperature distributions and velocity fields in the human eye exposed to EM fields in different body positions. In order to gain insight into the effects of body position on natural convection within the anterior chamber during exposure to EM fields, effects of an ambient temperature variation and thermoregulation were neglected. The ambient temperature was set to the human body temperature of 37°C. The convective coefficient due to the blood flow inside the sclera was set to $65 \, W/m^2 \cdot K$ [14].

Form the simulation of the 900 MHz frequency, the EM energy absorbed (SAR) is the highest over the front part of the eye (Figure 5a), corresponding to its large temperature gradient (Figure 5b). However, for the 1,800 MHz frequency, it is observed that a large temperature gradient is significantly produced by the EM energy absorbed (Figure 6a) at the middle part of the eyeball (Figure 6b). For the middle part of the eye, the temperature profile for each body position is almost the same. The temperature profiles especially within the vitreous for three different body positions are closer to each other for both 900 and 1,800 MHz frequencies. It means that body position has little effect on heat transfer in the middle part of the eye when exposed to EM fields. However, the body position still plays an important role on AH natural convection and the heat transfer process within the anterior chamber and its periphery in the front part of the eye.

The effect of body position on velocity field in the eye during exposure to EM fields in different body positions is shown in Figures 5c and 6c. When the human eye subjected to EM fields, the AH motion in the anterior chamber occurs mainly by natural means such as buoyancy. Since the AH velocity associated with natural convection is relatively low, the heat transfer coefficient encountered in natural convection is also low. This is because the velocity fields vary corresponding to the temperature gradient in the eye. At the peripheral region of the anterior chamber where the convection flow is small, temperature distributions are primarily governed by the conduction mode. Within the anterior chamber, in the case of a lower temperature gradient, the circulatory patterns have a lower speed, where a circulatory pattern with a higher temperature gradient flows faster. Besides the temperature gradient, the changes in body position that change the anterior chamber orientation have a significant effect on the AH natural convection. Figures 5c and 6c show the circulatory patterns in the anterior chamber in the eye in different body positions during exposure to the EM frequencies of 900 and 1,800 MHz, respectively.

*In sitting position* velocity field of the 900 MHz (Figure 5c) flow is slower than that of 1,800 MHz (Figure 6c), but the 900 MHz case has a more complex motion. The natural convection of the 900 MHz forms the two circulatory patterns with opposite direction in the anterior chamber (Figure 5c). These patterns imply that the generated heat is transferred in two directions: one is to the corneal surface and the other is to the lens surface. While in the 1,800 MHz, the velocity field becomes faster and the flow circulates in the counterclockwise direction (Figure 6c). It is implied that the heat transfer travels outward from the lens surface to the corneal surface. *In the supine position*, double circulation cells are formed. The flow patterns are symmetrical between the left and right sides for both 900 and 1,800 MHz frequencies, but in case of 900 MHz the flow is faster. The primary circulation flows in a counterclockwise direction, whereas the secondary circulation flows in a clockwise direction. This seems to imply that the heat transfers are both traveling outward rising from the lens surface. *In the prone position*, again the two circulatory cells are formed with the opposite direction in the anterior chamber, but in a counter-current direction to the flow of the supine position. Heat flow direction in the anterior chamber changes from outward convection to inward convection with repositioning of the body position from supine to prone.

Figures 7 and 8 illustrate the temperature profile in the front part of the eye during exposure to EM frequencies of 900 and 1,800 MHz, respectively, in different body positions. With the domination of the AH natural convection, the heat transfer rate increases corresponding to the temperature gradient induced by EM fields. In both 900 and 1,800 MHz, the maximum temperatures in the anterior chamber are presented in the supine position. This is due to the fact that the localized heating of the AH near the corneal surface on the top position of the anterior chamber cannot easily be released by the physical mechanism of natural convection. Moreover, there are small differences in the temperature
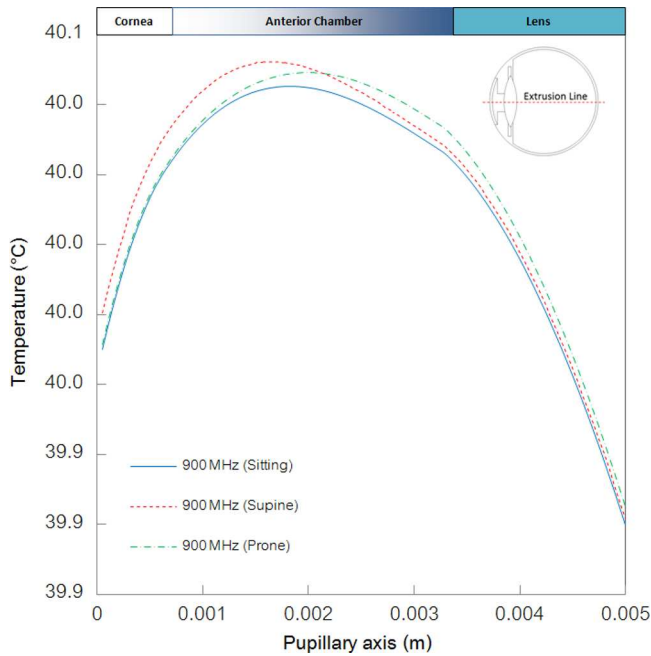
**Figure 7.** Temperature profile versus papillary axis of the eye exposed to the EM frequency of 900 MHz at 60 minutes.

profiles of sitting, supine, and prone in the lens region due to the domination of conduction heat transfer. However, there are is a huge difference between each body position on the temperature profile in the anterior chamber region, especially at 900 MHz (Figure 7) due to the domination of the difference in the AH natural convection behavior.
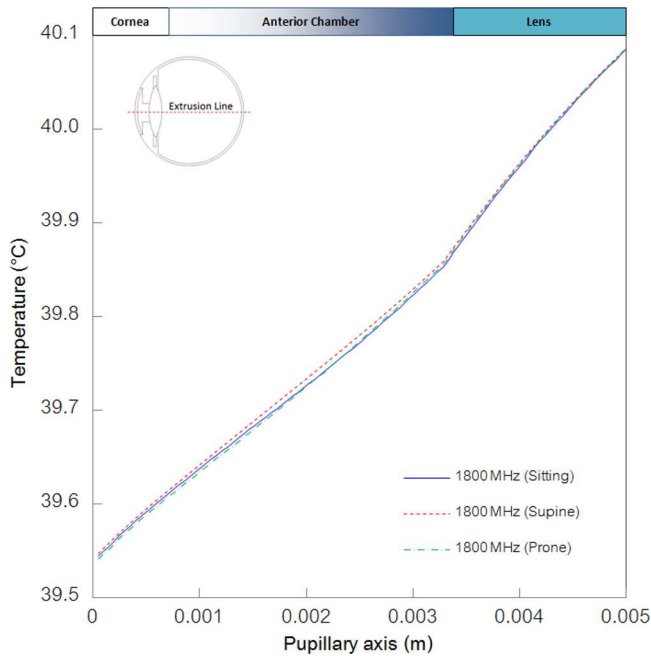


**Figure 8.** Temperature profile versus papillary axis of the eye exposed to the EM frequency of 1,800 MHz at 60 minutes.

As a result, it can be concluded that the gravity effects on the AH flow and heat transfer have a different effect depending on the eye orientation, which is relative to the body position. The effect of body position becomes more significant on heat transfer in the front part of the eye where the AH flow exists. This behavior is due to the fact that in the different body positions at the same EM exposure condition, the frontal eye temperature profile is not the same. This indicates that the AH natural convection behavior is different at different body positions for the same EM exposure condition.

## 5. Conclusions

A numerical analysis of the SAR, AH natural convection, and heat transfer in the eye during exposure to EM fields in different body positions has been performed. The results of the SAR values are increased corresponding to the electric field intensities. Besides the electric field intensity, the magnitude of the dielectric and thermal properties in each tissue will directly affect the SAR values in the eye. In this study, the AH natural convection of the human eye in different body positions induced by EM fields is systematically investigated. It is found that the AH natural convection increases on increasing the anterior chamber temperature gradient. The influence of AH natural convection is particularly strong in the front part of the eye. Body positions affect both AH velocity field and temperature distribution in the anterior chamber and the surrounding area. This is because the gravity effect on the AH flow and heat transfer has a different effect depending on the eye orientation, which is relative to the body position and the AH natural convection in the anterior chamber plays a significant role in transferring heat.

No remarkable change in the temperature increases in the middle part of the eye especially in the vitreous is observed with body repositioning. In this study, the difference in frontal eye temperature profile is caused by the heating pattern (EM frequency) and anterior chamber configuration (body position), which become the dominant mechanisms for the AH natural convection. The obtained results contribute to the understanding of the realistic situation and prediction of the temperature distribution within the eye during exposure to EM fields.

## Funding

## References

[1] T. Wessapan and P. Rattanadecho, Specific Absorption Rate and Temperature Increase in Human Eye Subjected to Electromagnetic Fields at 900 MHz, *ASME J. Heat Transfer*, vol. 134, p. 091101, 2012.

[2] T. Wessapan and P. Rattanadecho, Specific Absorption Rate and Temperature Increase in the Human Eye due to Electromagnetic Fields Exposure at Different Frequencies, *Int. J. Heat Mass Transfer*, vol. 64, pp. 426–435, 2013.

[3] T. Wessapan and P. Rattanadecho, Influence of Ambient Temperature on Heat Transfer in the Human Eye during Exposure to Electromagnetic Fields at 900 MHz, *Int. J. Heat Mass Transfer*, vol. 70, pp. 378–388, 2014.

[4] International Commission on Non-Ionizing Radiation Protection (ICNIRP), Guidelines for Limiting Exposure to Time-Varying Electric, Magnetic and Electromagnetic Fields (up to 300 GHz), *Health Phys.*, vol. 74, pp. 494–522, 1998.

[5] IEEE, IEEE Standard for Safety Levels with Respect to Human Exposure to Radio Frequency Electromagnetic Fields, 3 kHz to 300 GHz (1999), IEEE Standard C95 1–1999.

[6] J. J. W. Lagendijk, A Mathematical Model to Calculate Temperature Distribution in Human and Rabbit Eye During Hyperthermic Treatment, *Phys. Med. Biol.*, vol. 27, pp. 1301–1311, 1982.

[7] J. Scott, A Finite Element Model of Heat Transport in the Human Eye, *Phys. Med. Biol.*, vol. 33, pp. 227–241, 1988.

[8] T. Wu, P. Li, Q. Shao, J. Hong, L. Yang, and S. Wu, A Simulation-Experiment Method to Characterize the Heat Transfer in Ex-Vivo Porcine Hepatic Tissue with a Realistic Microwave Ablation System, *Numer. Heat Transfer, Part A*, vol. 64, pp. 729–743, 2013.

[9] E. H. Amara, Numerical Investigations on Thermal Effects of Laser–Ocular Media Interaction, *Int. J. Heat Mass Transfer*, vol. 38, pp. 2479–2488, 1995.

[10] A. Hirata, S. Matsuyama, and T. Shiozawa, Temperature Rises in the Human Eye Exposed to EM Waves in the Frequency Range 0.6–6 GHz, *IEEE Trans. Electromagn. Compat.*, vol. 42, no. 4, pp. 386–393, 2000.

[11] K. J. Chua, J. C. Ho, S. K. Chou, and M. R. Islam, On the Study of the Temperature Distribution within a Human Eye Subjected to a Laser Source, *Int. Commun. Heat Mass Transfer*, vol. 32, pp. 1057–1065, 2005.

[12] W. Limtrakarn, S. Reepolmaha, and P. Dechaumphai, Transient Temperature Distribution on the Corneal Endo-thelium during Ophthalmic Phacoemulsification: A Numerical Simulation Using the Nodeless Variable Element, *Asian Biomed.*, vol. 4, no. 6, pp. 885–892, 2010.

[13] S. Kumar, S. Acharya, R. Beuerman, and A. Palkama, Numerical Solution of Ocular Fluid Dynamics in a Rabbit Eye: Parametric Effects, *Ann. Biomed. Eng.*, vol. 34, pp. 530–544, 2006.

[14] E. Ooi and E. Y. K. Ng, Simulation of Aqueous Humor Hydrodynamics in Human Eye Heat Transfer, *Comput. Biol. Med.*, vol. 38, pp. 252–262, 2008.

[15] E. H. Ooi and E. Y. K. Ng, Effects of Natural Convection Inside the Anterior Chamber, *Int. J. Numer. Methods Biomed. Eng.*, vol. 27, pp. 408–423, 2011.

[16] H. H. Pennes, Analysis of Tissue and Arterial Blood Temperatures in the Resting Human Forearm, *J. Appl. Physiol.*, vol. 1, pp. 93–122, 1948.

[17] H. H. Pennes, Analysis of Tissue and Arterial Blood Temperatures in the Resting Human Forearm, *J. Appl. Physiol.*, vol. 85, no. 1, pp. 5–34, 1998.

[18] V. M. M. Flyckt, B. W. Raaymakers, and J. J. W. Lagendijk, Modeling the Impact of Blood Flow on the Tempera-ture Distribution in the Human Eye and the Orbit: Fixed Heat Transfer Coefficients Versus the Pennes Bioheat Model Versus Discrete Blood Vessels, *Phys. Med. Biol.*, vol. 51, pp. 5007–5021, 2006.

[19] E. Y. K. Ng and E. H. Ooi, FEM Simulation of the Eye Structure with Bioheat Analysis, *Comput. Methods Programs Biomed.*, vol. 82, pp. 268–276, 2006.

[20] E. H. Ooi and E. Y. K. Ng, Ocular Temperature Distribution: A Mathematical Perspective, *J. Mech. Med. Biol.*, vol. 9, pp. 199–227, 2009.

[21] A. Nakayama and F. Kuwahara, A General Bioheat Transfer Model Based on the Theory of Porous Media, *Int. J. Heat Mass Transfer*, vol. 51, pp. 3190–3199, 2008.

[22] P. Keangin, K. Vafai, and P. Rattanadecho, Electromagnetic Field Effects on Biological Materials, *Int. J. Heat Mass Transfer*, vol. 65, pp. 389–399, 2013.

[23] K. Khanafer and K. Vafai, Synthesis of Mathematical Models Representing Bioheat Transport, *Adv. Numer. Heat Transfer*, vol. 3, pp. 1–28, 2009.

[24] M. Shafahi and K. Vafai, Human Eye Response to Thermal Disturbances, *ASME J. Heat Transfer*, vol. 133, p. 011009, 2011.

[25] E. Y. K. Ng, J. H. Tan, U. R. Acharya, and J. S. Suri, *Human Eye Imaging and Modeling*, CRC Press, Florida, 2012. ISBN: 978-1-4398-6993-2.

[26] D. Sumeet, U. R. Acharya, and E. Y. K. Ng, *Computational Analysis of Human Eye with Application*, WSPC Press, Singapore, 2011. ISBN: 978-981-4340-29-8.

[27] E. Y. K. Ng, U. R. Acharya, J S. Suri, and A. Campilho, *Image Analysis and Modeling in Ophthalmology*, CRC Press, Florida, 2014. ISBN: 978-1-4665-5930-1.

[28] E. Y. K. Ng, U. R. Acharya, R. M. Rangayyan, and J. S. Suri, *Ophthalmology Imaging and Applications*, CRC Press, Florida, 2014. ISBN: 978-1-4665-5913-4.

[29] E. H. Ooi, W. T. Ang, and E. Y. K. Ng, A Boundary Element Model of the Human Eye Undergoing Laser Thermokeratoplasty, *Comput. Biol. Med.*, vol. 28, pp. 727–738, 2008.

[30] E. H. Ooi, W. T. Ang, and E. Y. K. Ng, A Boundary Element Model for Investigating the Effects of Eye Tumor on the Temperature Distribution inside the Human Eye, *Comput. Biol. Med.*, vol. 28, pp. 727–738, 2009.

[31] J. H. Tan, E. Y. K. Ng, U. R. Acharya, and C. Chee, Study of Normal Ocular Thermogram Using Textural Parameters, *Infrared Phys. Technol.*, vol. 53, pp. 120–126, 2010.

[32] J. H. Tan, E. Y. K. Ng, and U. R. Acharya, Evaluation of Tear Evaporation from Ocular Surface by Functional Infrared Thermography, *Med. Phys.*, vol. 37, pp. 6022–6034, 2010.

[33] J. H. Tan, E. Y. K. Ng, and U. R. Acharya, Evaluation of Topographical Variation in Ocular Surface Temperature by Functional Infrared Thermography, *Infrared Phys. Technol.*, vol. 54, pp. 469–477, 2011.

[34] N. Heussner, L. Holl, T. Nowak, T. Beuth, M. S. Spitzer, and W. Stork, Prediction of Temperature and Damage in an Irradiated Human Eye—Utilization of a Detailed Computer Model Which Includes a Vectorial Blood Stream in the Choroid, *Comput. Biol. Med.*, vol. 51, pp. 35–43, 2014.

[35] T. Wessapan, S. Srisawatdhisukul, and P. Rattanadecho, Numerical Analysis of Specific Absorption Rate and Heat Transfer in the Human Body Exposed to Leakage Electromagnetic Field at 915 MHz and 2450 MHz, *ASME J. Heat Transfer*, vol. 133, p. 051101, 2011.

[36] T. Wessapan, S. Srisawatdhisukul, and P. Rattanadecho, The Effects of Dielectric Shield on Specific Absorption Rate and Heat Transfer in the Human Body Exposed to Leakage Microwave Energy, *Int. Commun. Heat Mass Transfer*, vol. 38, pp. 255–262, 2011.

[37] T. Wessapan and P. Rattanadecho, Numerical Analysis of Specific Absorption Rate and Heat Transfer in Human Head Subjected to Mobile Phone Radiation, *ASME J. Heat Transfer*, vol. 134, p. 121101, 2012.

[38] T. Wessapan, S. Srisawatdhisukul, and P. Rattanadecho, Specific Absorption Rate and Temperature Distributions in Human Head Subjected to Mobile Phone Radiation at Different Frequencies, *Int. J. Heat Mass Transfer*, vol. 55, pp. 347–359, 2012.

[39] P. Keangin, T. Wessapan, and P. Rattanadecho, Analysis of Heat Transfer in Deformed Liver Cancer Modeling Treated Using a Microwave Coaxial Antenna, *Appl. Therm. Eng.*, vol. 31, no. 16, pp. 3243–3254, 2011.

[40] P. Keangin, T. Wessapan, and P. Rattanadecho, An Analysis of Heat Transfer in Liver Tissue during Microwave Ablation Using Single and Double Slot Antenna, *Int. Commun. Heat Mass Transfer*, vol. 38, pp. 757–766, 2011.

[41] P. Rattanadecho and P. Keangin, Numerical Study of Heat Transfer and Blood Flow in Two-Layered Porous Liver Tissue During Microwave Ablation Process Using Single and Double Slot Antenna, *Int. J. Heat Mass Transfer*, vol. 58, pp. 457–470, 2013.

[42] P. Bernardi, M. Cavagnaro, S. Pisa, and E. Piuzzi, Specific Absorption Rate and Temperature Increases in the Head of a Cellular-Phone User, *IEEE Trans. Microw. Theor. Tech.*, vol. 48, no. 7, pp. 1118–1126, 2000.

[43] S. Park, J. Jeong, and Y. Lim, Temperature Rise in the Human Head and Brain for Portable Handsets at 900 and 1800 MHz, *Proceedings of the Fourth International Conference on Microwave and Millimeter Wave Technology*, vol. 1, pp. 966–969, 2004.